Mitochondrial dysfunction generates a growth-restraining signal linked to pyruvate in *Drosophila* larvae

Jack George, Tea Tuomela, Esko Kemppainen, Antti Nurminen,

Samuel Braun, Cagri Yalgin & Howard T. Jacobs

SUPPLEMENTARY DATA

SUPPLEMENTARY FIGURE LEGENDS

Figure S1

Specificity of the various GAL4 drivers used in the experiments

Micrographs of adult and developing flies of the stages indicated, expressing GFP either as UAS-Stinger (Stinger, nuclear-localized) or UAS-mCD8-GFP (mCD8, membrane localized) under the control the indicated drivers (see Table 2). (A) Larvae, L1, L2 - the first two larval instars, (B-E) L3 larvae, (F) pupae and (G) adults or specific structures thereof. The observed patterns broadly conform with those reported in the literature. (H-K) Further analysis of the specificity of the *nrv2*-GAL4 driver. The *nrv2*-GAL4 driver has been reported to drive expression in glial cells and in some neurons, although the literature is not fully consistent (see refs. 33-37), prompting us to re-examine the issue in relation to both the brain and the PNS. (H) Single optical sections of the whole adult brain, co-immunostained for GFP (Stinger) driven by *nrv2*-GAL4 (green, Alexa 488 label), and for elav (far red, Alexa 647, avoiding bleeding between channels), with insets of the same images shown at higher magnification in (I). Also shown in (H, image iv) is a 'reciprocal image' of Stinger expression driven by neuronal driver *elav*-GAL4, counterstained for the glial marker repo, showing no overlap. Cells showing the highest *nrv2*-GAL4 driven GFP expression in (I), e.g. those arrowed in white, are generally negative for elav, consistent with their being glial cells. However, some cells showing faint nuclear green fluorescence appear to be elav-positive, implying that they are neuronal. Note that many of them, such as those arrowed in red, are artefacts, due to strong fluorescence in adjacent z-layers. In trial experiments we could not exclude that the very faint fluorescence signal of some cells may be due to cross-reaction of the secondary antibodies; but using settings that exclude this very faint signal, we still found approximately 15% of faintly GFP-positive nuclei were still positive for elav (>150 individual GFP-positive nuclei examined, examples shown in J). (K) In the larval cuticle, strong *nrv2*-GAL4-directed nuclear GFP expression coincides with a subset of cells also expressing the glial marker repo (upper panels). Note that images shown here in (B) and (C) were also included in supplementary online data for Kemppainen *et al*., 2016 [7], but are reproduced here for convenience.

Figure S2

Confounding effect of TM3 balancer

Since we used marked balancer chromosomes extensively in the experiments, we conducted test crosses without any transgene, driver or RNAi, to establish whether these chromosomes alone conferred a developmental delay or its rescue, in the tko^{25t} background. (A, B) Time to eclosion (means $\pm$ SD, $n \geq 3$ vials in each cross) of flies of the indicated genotypes. Horizontal lines denoted by asterisks (*, ***) indicate significantly different groups in pairwise comparisons (Student's *t* test, $p < 0.05$, 0.001, respectively). The CyO balancer (A) for chromosome 2 did not affect eclosion timing, whilst the TM3*Sb* balancer for chromosome 3 (B) conferred a significant, additional developmental delay upon tko^{25t} flies. The effect was also seen in both sexes at 22 °C, or using TM3 combined instead with the *Ser* marker. We therefore advise that TM3 balancers should be avoided in experiments measuring developmental delay in tko^{25t}. Note also that the FM7 balancer causes a developmental delay in wild-type males. Use of a true wild-type control is therefore advisable, to quantify the extent of developmental delay in males. The bang-sensitive tko^{25t} phenotype was also exacerbated (D) by TM3Sb, but not by CyO (C), as shown by box-plots of recovery time: thick black bars indicate medians and upper and lower edges of the boxes indicate first and third quartiles, respectively, of progeny flies of the genotypes as indicated. Although it affects eclosion timing, FM7 does not produce bang-sensitivity in wild-type males. Note that all flies in these experiments were progeny from crosses of the general scheme tko^{25t} / FM7 ; balancer / + x tko^{25t} / Y.

Figure S3

Additive effects of tko^{+} rescue of tko^{25t} developmental delay by multiple drivers

(A) Time to eclosion (means $\pm$ SD, $n \geq 3$ replicate vials for each cross), of flies of the indicated inferred genotypes, using UAS-tko^{+}(8) with the indicated combination of drivers. Controls were FM7 balancer flies lacking transgene or G14. Horizontal lines denoted by asterisks (**) indicate significant differences in pairwise comparisons of flies of a given sex and *tko* genotype , with and without tko^{+} driven by the combined drivers, (Student's *t* test, $p < 0.01$. (B) For comparison, the length of developmental delay

conferred by *tko*^{25t} either alone, or in combination with UAS-tko+(8) with the indicated drivers. Despite the trend seen in both sexes, we do not consider it meaningful to implement a statistical analysis on these data, because they were derived from separate crosses. Note that the data using the combined drivers is from the experiment shown in (A) and that for *tko*^{25t} alone from the *Lsp2*-GAL4 cross.

Figure S4

Supplementary data on RNAi-mediated knockdown of malic enzyme isogenes

(A, B) Time to eclosion of flies of the indicated genotypes (i.e. with relevant *Men* or *Men-b* RNAi construct or balancer as shown); means $\pm$ SD, n $\geq$ 3 vials from each cross, at the indicated temperature (25 or 29 °C). Eclosion timing for *Men* RNAi at the alternative temperature was qualitatively similar for each cross, as shown in Fig. 7B. Horizontal bars denoted by asterisks (**) indicate significant differences, in pairwise comparisons of RNAi and balancer control flies of each given genotype and sex analyzed (Student's *t* test, $p < 0.001$). (C) Proportion (%) of eclosing RNAi male progeny that also carried *tko*^{25t}, as opposed to the FM7 balancer, from crosses of the general type: *tko*^{25t} / FM7 ; daGAL4 x FM7 / Y ; *Men-b* RNAi. Asterisks (***) above the bars denotes significant deviation from expected frequency of 50% (chi-squared test with Yates' continuity correction, $p < 0.001$).

Figure S5

Reports of statistical analysis of effects of drugs targeting pyruvate metabolism

Data from the experiment shown in Fig. 5A were analysed by 2-way ANOVA (online tool: vassartstats.net/anova2u.html), to determine the effects on eclosion timing of genotype (Oregon R wild-type v. *tko*^{25t}), drug (no drug, pyruvate, DCA or UK-5099) or the interaction between them.
The data were analysed separately within sexes and diets, and for the different drugs, producing the outputs as shown applying the Tukey HSD test where appropriate, to determine the source of variation. The findings are summarized in the main text.

Figure S6

Reports of statistical analysis of effects of RNAi targeted on pyruvate metabolism

Data from the experiment shown in Fig. 6B were analysed by 2-way ANOVA (online tool: vassartstats.net/anova2u.html), to determine the effects on eclosion timing of genotype (Oregon R wild-type v. tko^{25t}), RNAi (RNAi v. balancer control) or the interaction between them. The data were analysed separately within sexes and on media with or without pyruvate supplementation, and for the different targets *Mpc1* and *Pdk*, producing the outputs as shown applying the Tukey HSD test where appropriate, to determine the source of variation. The findings are summarized in the main text.

SUPPLEMENTARY TABLES

Supplementary Table S1

Alleviation of *tko*^{25t} developmental delay by UAS-tko^{+}(8) with various GAL4 drivers

Driver	**Temperature**[1]	**Males**	**Females**	**Comment**
gut-GAL4	18	**	***	partly from [7]
gut-GAL4	22	**	***	partly from [7] deleterious to wild-type flies
gut-GAL4	25	**	**	deleterious to wild-type flies
Lsp2-GAL4	29	ns	ns	
Lsp2-GAL4	26	ns	ns	
Lsp2-GAL4	22	**	***	Fig. 1A
Lsp2-GAL4	18	ns	**	
Mef2-GAL4	29	nd	ns	semilethal, lethal to males
Mef2-GAL4	26	ns	ns	semilethal
Mef2-GAL4	22	ns	*	semilethal
Mef2-GAL4	18	**	**	male semilethal, Fig. 1B
G14	29	nd	nd	lethal
G14	26	***	ns	

G14	22	***	*	Fig. 1C
G14	18	*	**	
elav-GAL4	29	nd	nd	lethal
elav-GAL4	26	**	**	male semilethal
elav-GAL4	22	**	**	Fig. 1D
elav-GAL4	18	**	***	

[1]Most GAL4 drivers exhibit the classic pattern of temperature dependence [9], i.e. increased activity at higher temperature. For the strongest drivers this may also lead to deleterious effects of over-expression at high temperature, such that a lower temperature produces optimal effects.

Supplementary Table S2

Comparison of gene expression changes produced by high-sugar diet, pyruvate supplementation and the *tko*^{25t} mutation

(i) based on mass fraction (FPKM)[1]

Transcript Class[2]	**Concordance class[3]**	***tko*^{25t}, ZS + pyr v. ZS**	**wt, HS v. ZS**	***tko*^{25t} HS v. ZS**	**HS, *tko*^{25t} v. wt**	**ZS, *tko*^{25t} v. wt**	**ZS + pyr, *tko*^{25t} v. wt**
Protein-coding upregulated	altered in same direction by ≥ threshold FPKM	98	11	2	0	4	1
	altered in same direction by < threshold FPKM	7	22	3	2	1	0
	altered in opposite direction by ≥ threshold FPKM	0	2	5	20	10	48
	altered in opposite direction by < threshold FPKM	0	5	13	19	13	1
	Excluded by initial statistical filtering	57	122	139	121	134	112
	Total	162	162	162	162	162	162
Protein-coding downregulated	altered in same direction by ≥ threshold FPKM	5	9	1	1	8	3
	altered in same direction by < threshold FPKM	2	0	1	0	0	2

	altered in opposite direction by ≥ threshold FPKM	0	0	2	2	0	2
	altered in opposite direction by < threshold FPKM	0	0	0	3	0	1
	Excluded by initial statistical filtering	8	6	11	9	7	7
	Total	15	15	15	15	15	15
Non-coding upregulated	altered in same direction by ≥ threshold FPKM	1	0	0	0	0	0
	altered in same direction by < threshold FPKM	0	0	0	0	0	0
	altered in opposite direction by ≥ threshold FPKM	0	1	1	0	0	1
	altered in opposite direction by < threshold FPKM	0	0	0	0	0	0
	Excluded by initial statistical filtering	1	1	1	2	2	1
	Total	2	2	2	2	2	2
Non-coding downregulated	altered in same direction by ≥ threshold FPKM	15	1	0	0	6	0
	altered in same direction by < threshold FPKM	2	0	2	0	2	0

	altered in opposite direction by ≥ threshold FPKM	0	0	3	0	0	0
	altered in opposite direction by < threshold FPKM	0	0	3	0	0	0
	Excluded by initial statistical filtering	2	18	11	19	11	19
	Total	19	19	19	19	19	19

(ii) based on fold changes[4]

Transcript Class[2]	**Concordance class[3]**	***tko*^{25t}, ZS + pyr v. ZS**	**wt, HS v. ZS**	***tko*^{25t} HS v. ZS**	**HS, *tko*^{25t} v. wt**	**ZS, *tko*^{25t} v. wt**	**ZS + pyr, *tko*^{25t} v. wt**
Protein-coding upregulated	altered in same direction by ≥ threshold FPKM	56	7	1	0	2	0
	altered in same direction by < threshold FPKM	20	21	3	0	3	2
	altered in opposite direction by ≥ threshold FPKM	0	0	1	5	1	16
	altered in opposite direction by < threshold FPKM	0	0	6	18	5	20
	Excluded by initial statistical filtering	50	98	115	103	115	88
	Total	126	126	126	126	126	126

Protein-coding downregulated	altered in same direction by ≥ threshold FPKM	7	7	1	1	3	0
	altered in same direction by < threshold FPKM	3	4	9	3	5	0
	altered in opposite direction by ≥ threshold FPKM	0	0	0	1	3	2
	altered in opposite direction by < threshold FPKM	0	0	0	3	3	2
	Excluded by initial statistical filtering	8	7	8	10	4	14
	Total	18	18	18	18	18	18
Non-coding upregulated	altered in same direction by ≥ threshold FPKM	11	6	3	4	9	0
	altered in same direction by < threshold FPKM	2	0	1	4	0	1
	altered in opposite direction by ≥ threshold FPKM	2	0	2	1	1	9
	altered in opposite direction by < threshold FPKM	6	0	2	2	0	14
	Excluded by initial statistical filtering	21	36	34	31	32	18
	Total	42	42	42	42	42	42

Non-coding downregulated	altered in same direction by ≥ threshold FPKM	23	9	2	0	7	0
	altered in same direction by < threshold FPKM	14	3	6	5	19	1
	altered in opposite direction by ≥ threshold FPKM	2	0	2	5	0	7
	altered in opposite direction by < threshold FPKM	2	3	8	4	4	1
	Excluded by initial statistical filtering	21	47	44	48	32	53
	Total	62	62	62	62	62	62

Notes

1. Primary comparison was based on RNA-seq data from wt (wild-type, Oregon R) L3 larvae cultured in ZS medium supplemented with 25 mg/ml pyruvate, versus unsupplemented ZS medium. After the initial filter by Cuffdiff to exclude transcripts that were not significantly different between the two data sets, an arbitrary threshold of 100 FPKM was set, defining 162 upregulated and 15 downregulated protein-coding transcripts, plus 2 upregulated and 19 downregulated non-coding transcripts. The Table specifies how many transcripts of each class were altered concordantly or discordantly in the other comparisons, with the remainder excluded by the initial statistical filtering, as indicated.

2. Based on current genome annotations in flybase.

3. Out of the transcripts of that class from the primary comparison, totals as shown.

4. Primary comparison was based on RNA-seq data from wt (wild-type, Oregon R) L3 larvae cultured in ZS medium supplemented with 25 mg/ml pyruvate, versus unsupplemented ZS medium. After the initial statistical filter, an arbitrary threshold of 3 $\log_2$ units of fold change was set, defining 122 upregulated and 38 downregulated protein-coding transcripts, plus 37 upregulated and 44 downregulated non-coding transcripts. The Table specifies how many transcripts of each class were altered concordantly or discordantly in the other comparisons, with the remainder excluded by the initial statistical filtering, as indicated.

A

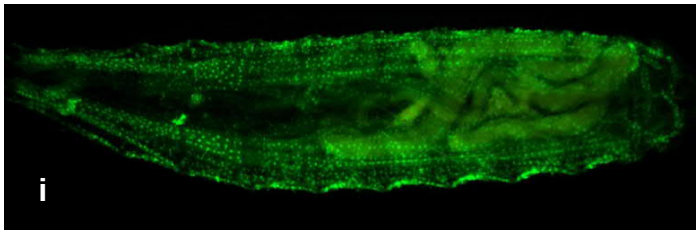

G14, L1, Stinger

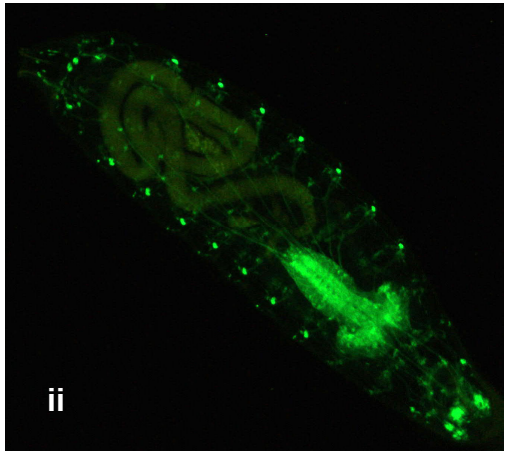

***elav*-GAL4, L1, mCD8**

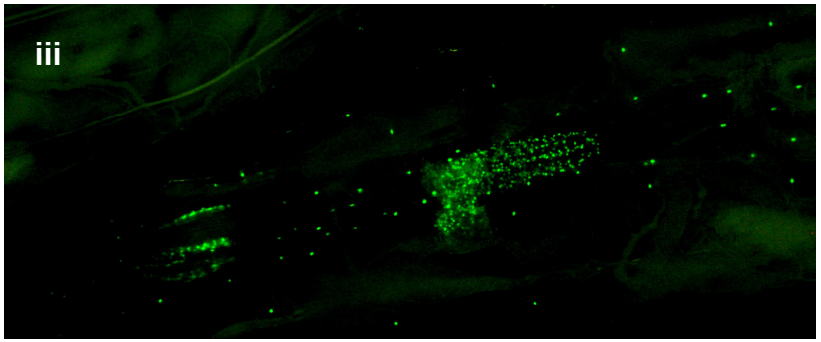

***nrv2*-GAL4, L2, Stinger**

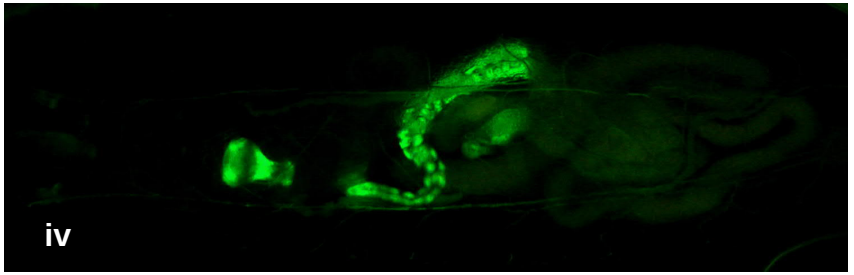

***Kr*-GAL4, L2, Stinger**

B

sg – salivary gland
mg – midgut
mt – Malpighian tubule
gc – gastric caeca
hg – hindgut
b – brain
c – carcass
id – imaginal discs

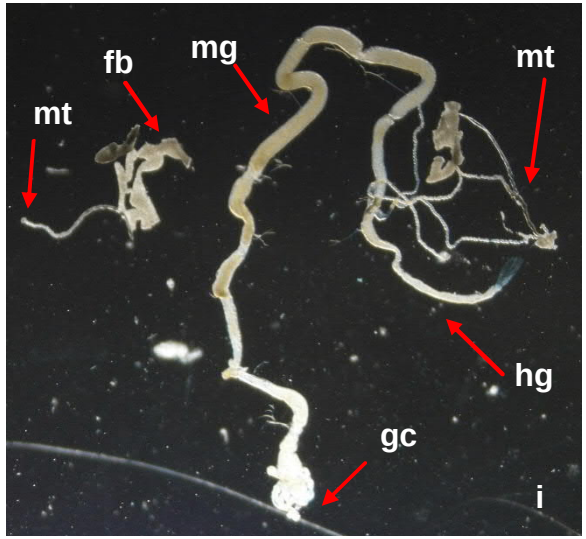

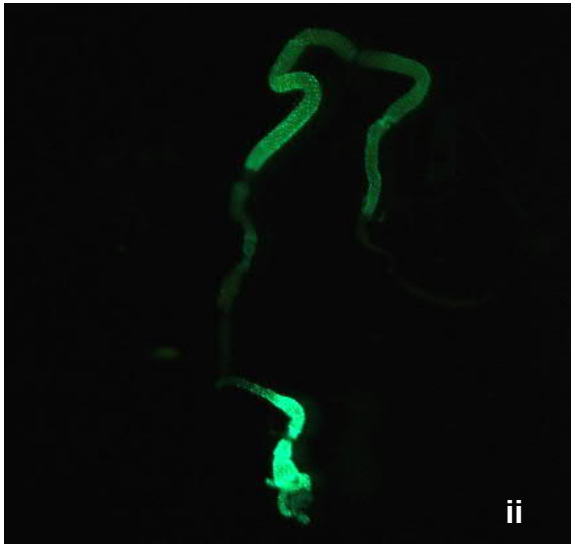

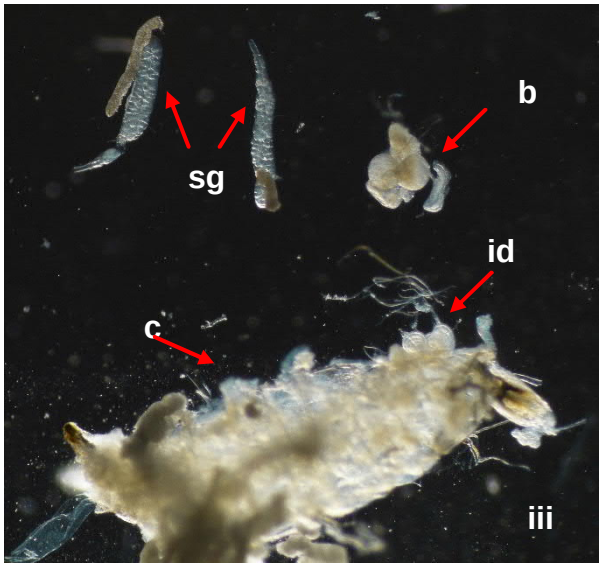

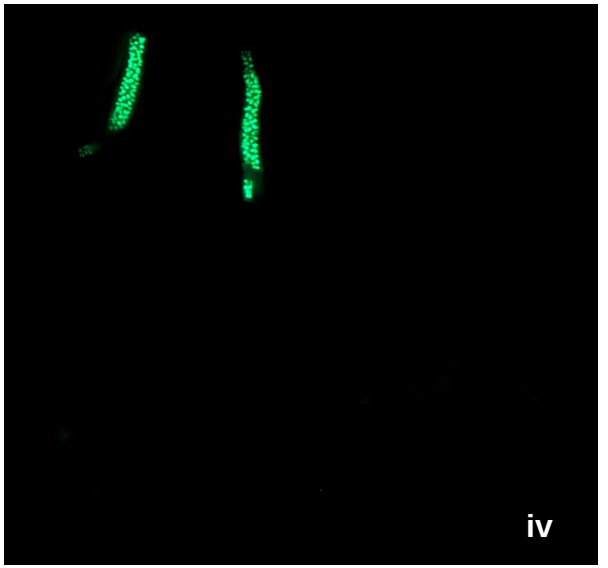

gut-GAL4, Stinger, dissected L3

C

gut-GAL4, Stinger, dissected L3

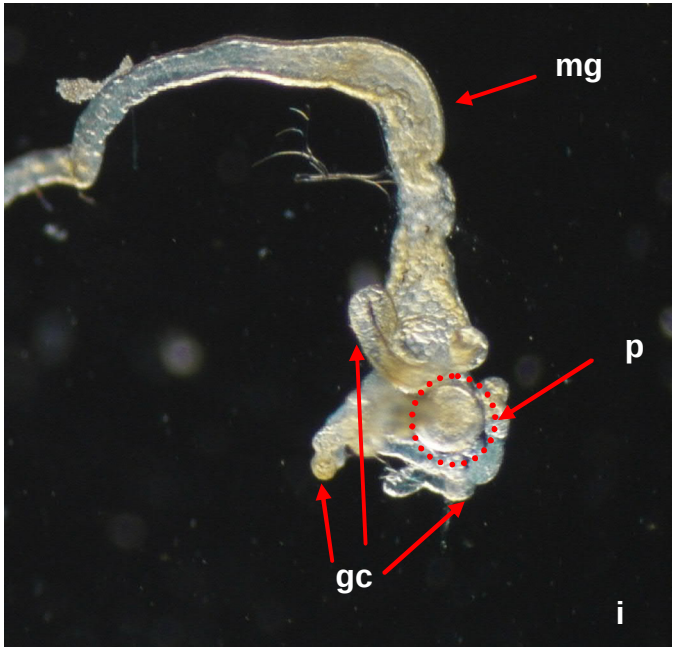

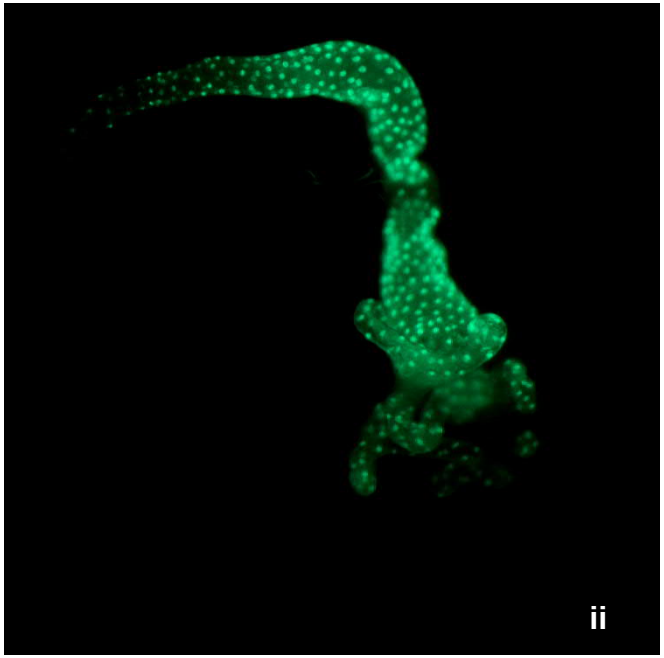

mg – midgut
p – proventricuulus
gc – gastric caeca

D

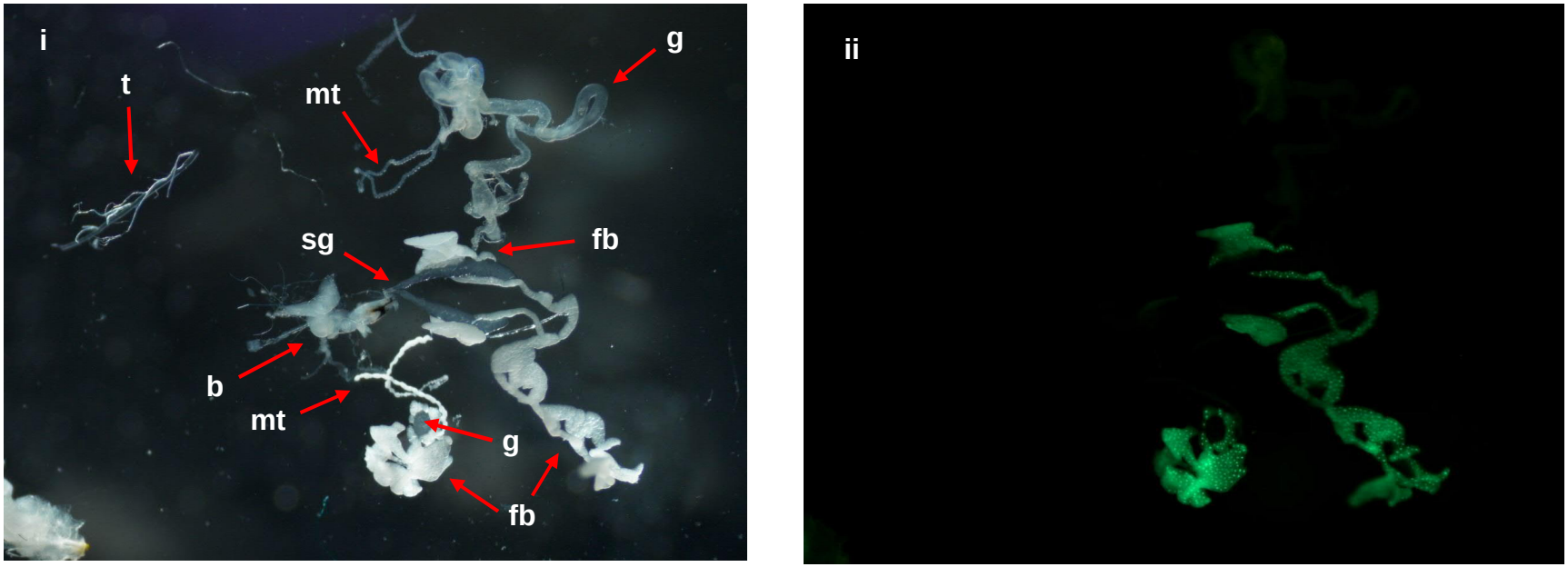

Lsp2-GAL4, Stinger, L3

sg – salivary gland
mt – Malpighian tubule
g – gonad
b – brain
c – carcass
t – trachaea
g – gut
fb – fat body

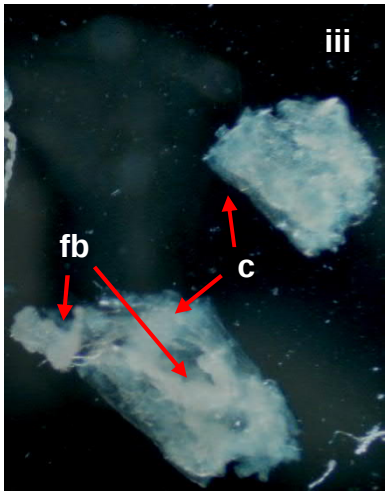

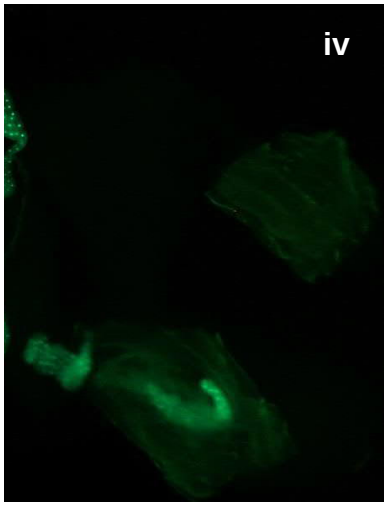

E

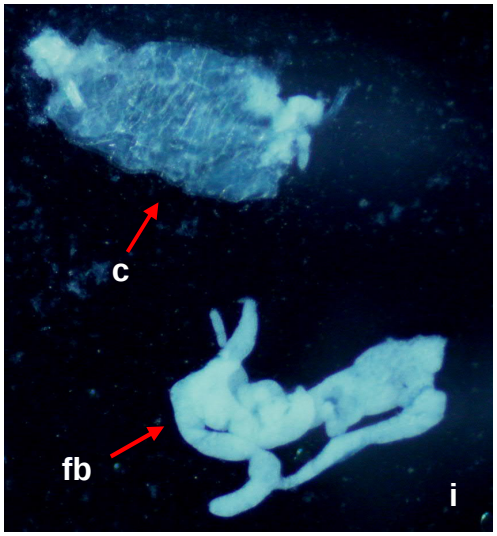

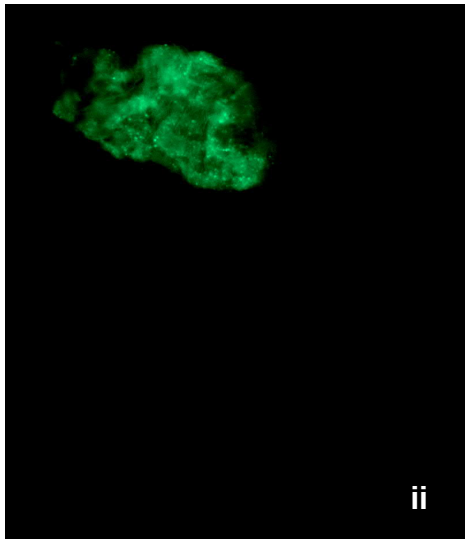

Mef2-GAL4, mCD8, L3

c – carcass
fb – fat body
t – trachaea
b – brain
mt – Malpighian tubule

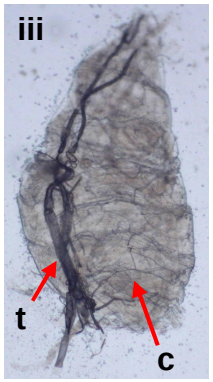

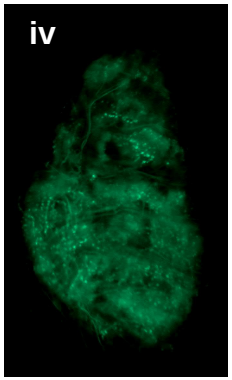

Mef2-GAL4,
Stinger, L3

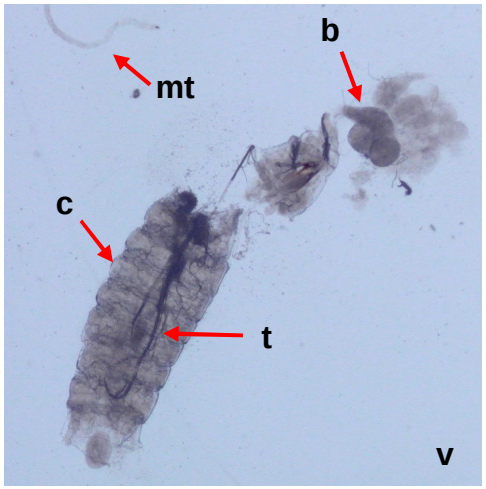

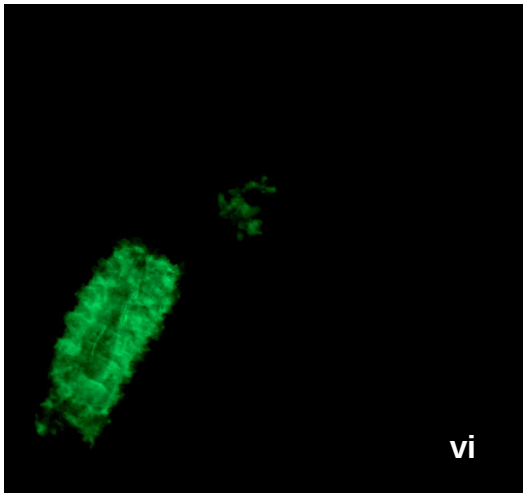

Mef2-GAL4, mCD8, L3

F

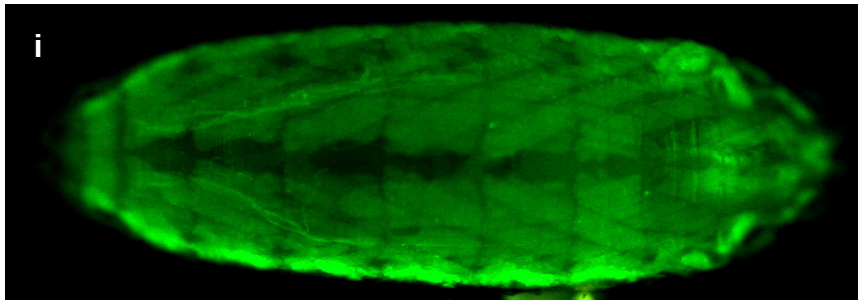

G14, mCD8

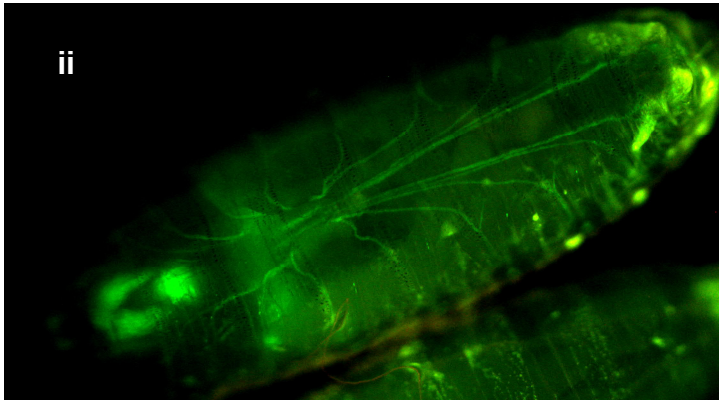

***elav*-GAL4, mCD8**

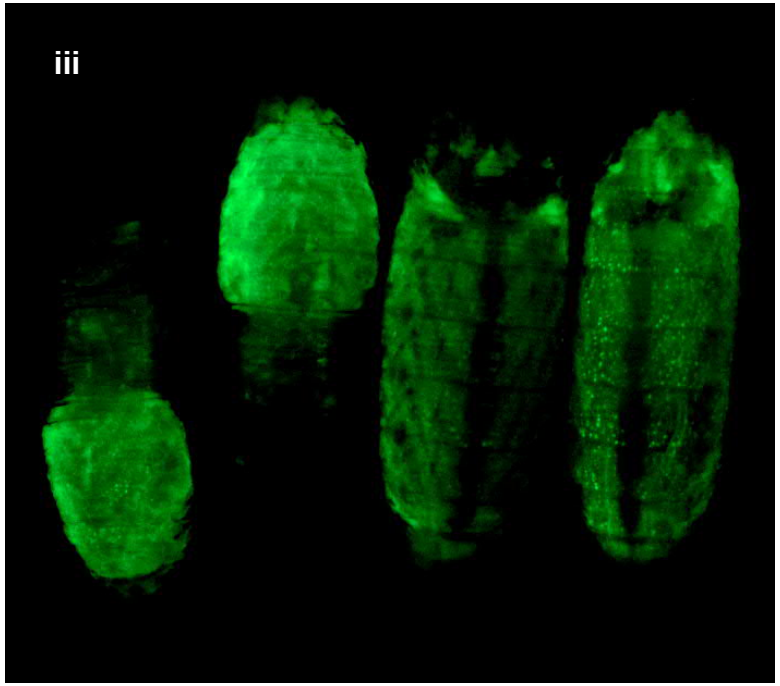

***Mef2*-GAL4 Stinger**

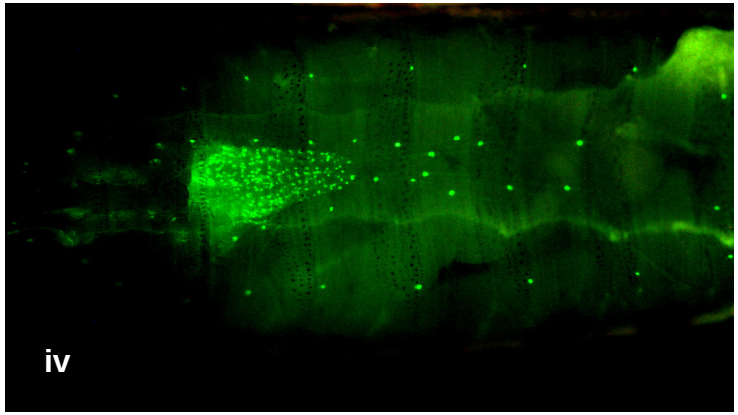

***nrv2*-GAL4, Stinger**

G

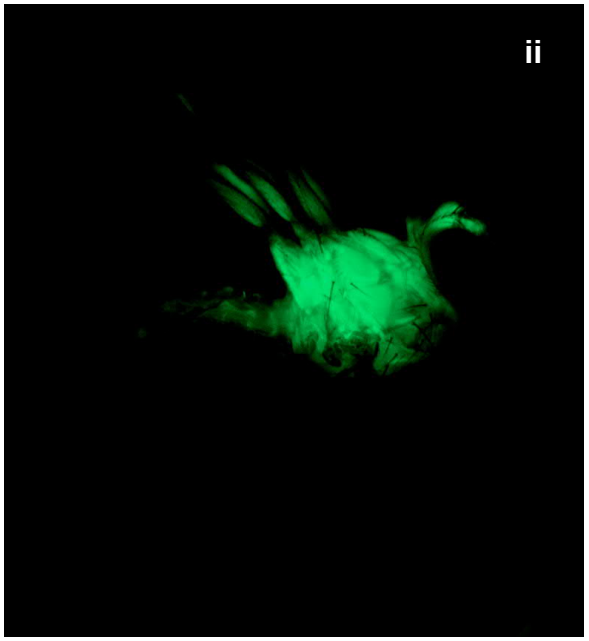

adult female

dissected adult thoracic muscles

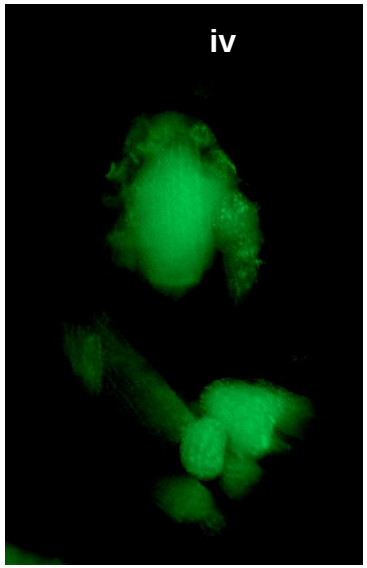

***Mef2*-GAL4, mCD8**

H

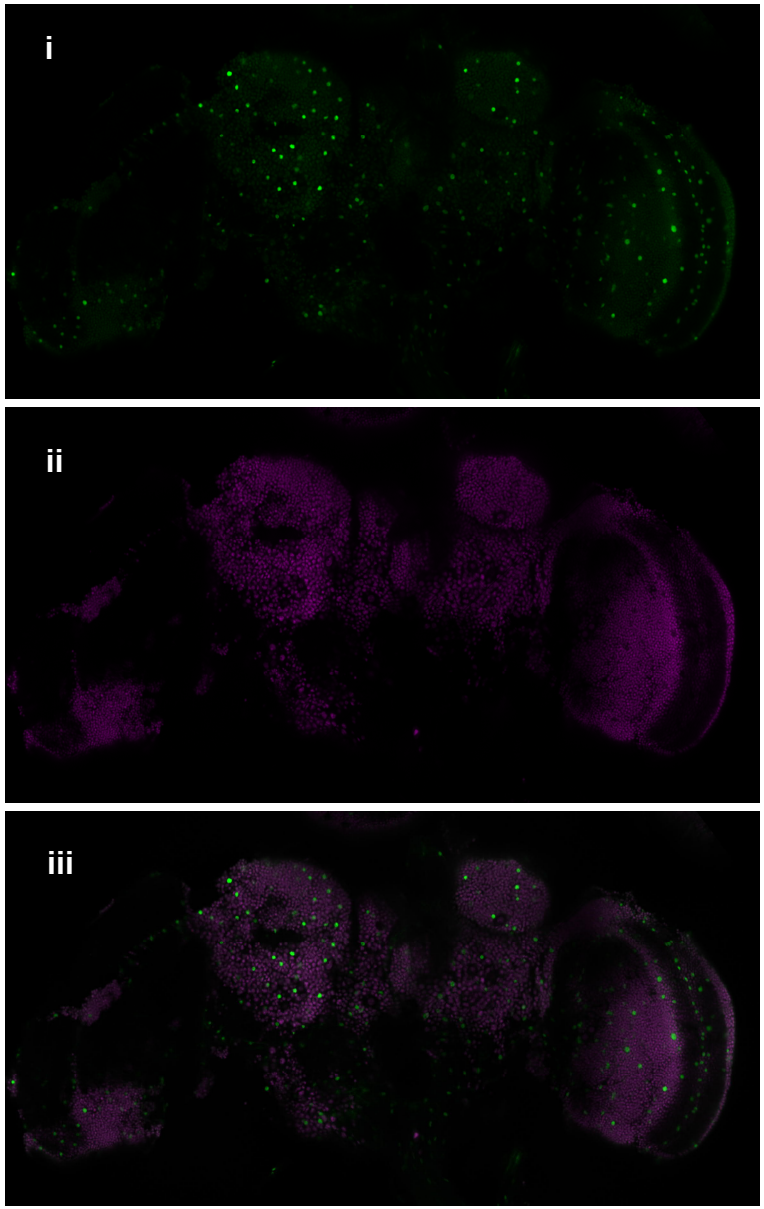

GFP

elav

merge

***nrv2*-GAL4, Stinger, adult brain**

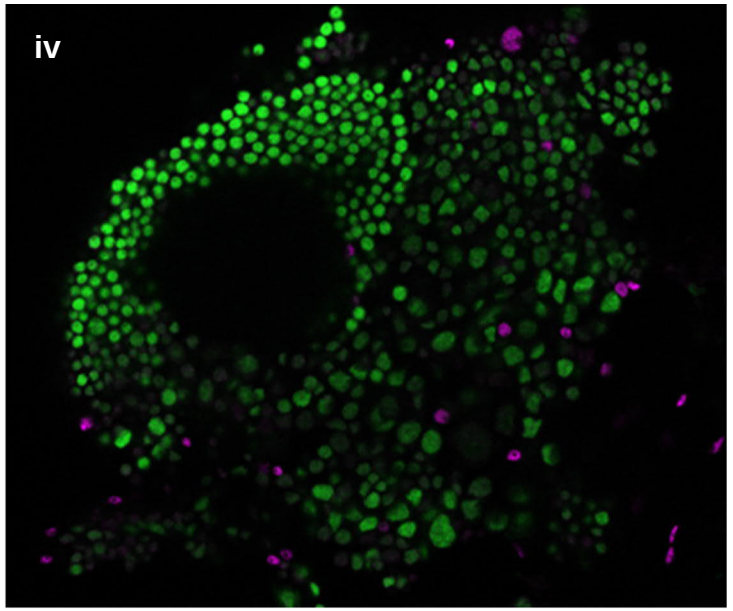

***elav*-GAL4, Stinger, adult brain counter-stained for repo**

I

nrv2-GAL4, Stinger, adult brain

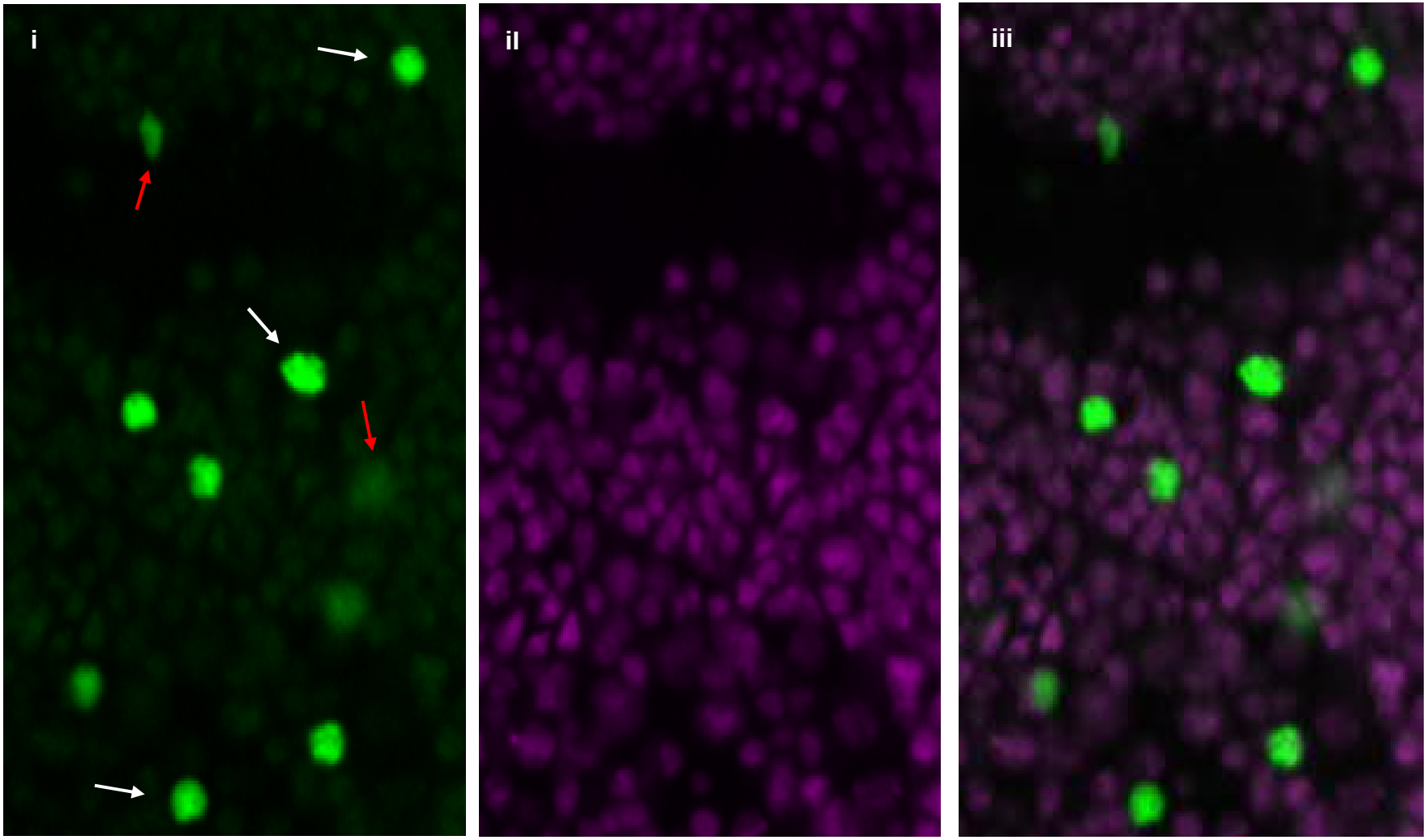

GFP elav merge

J

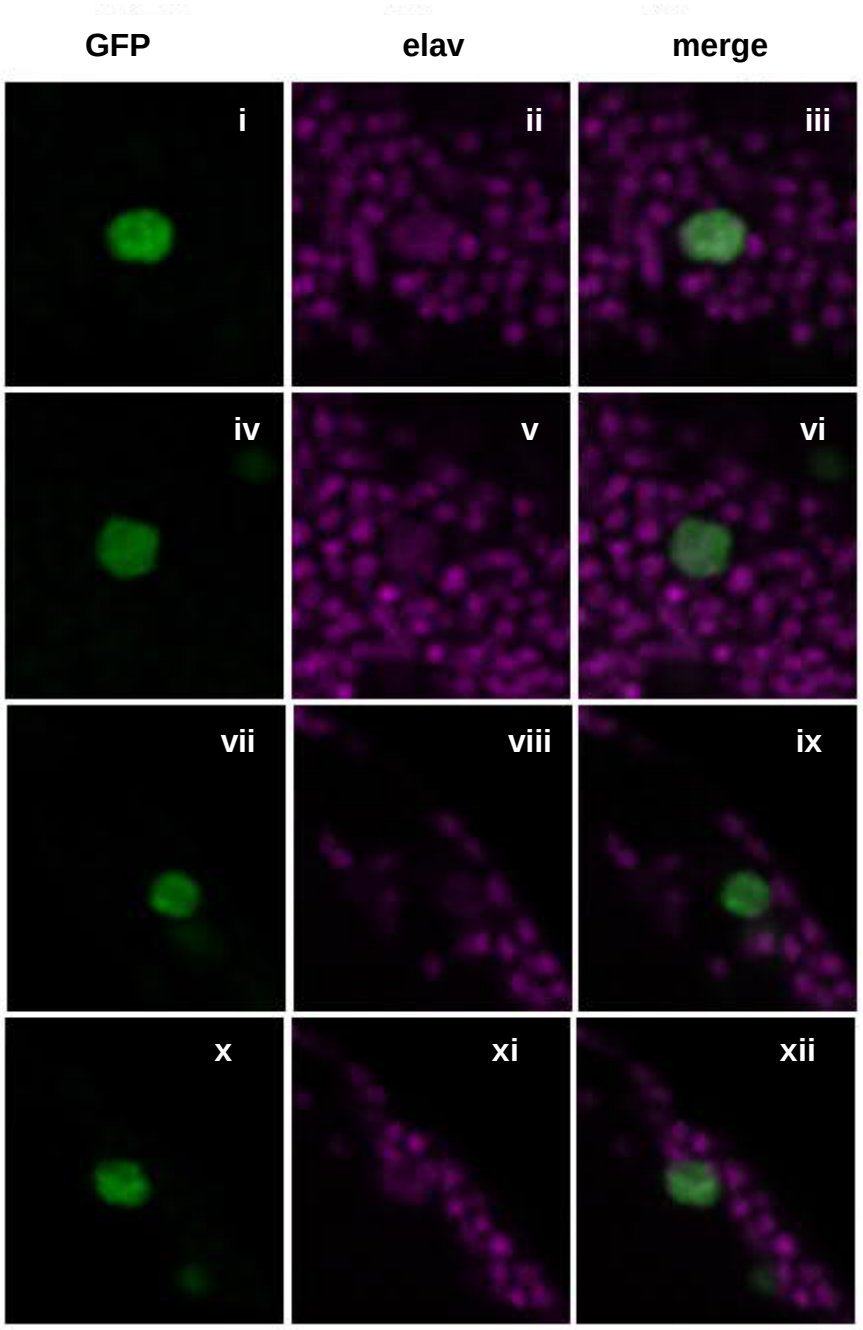

***nrv2*-GAL4, Stinger, adult brain, modified image capture settings**

K

***nrv2*-GAL4, Stinger, larval cuticle**

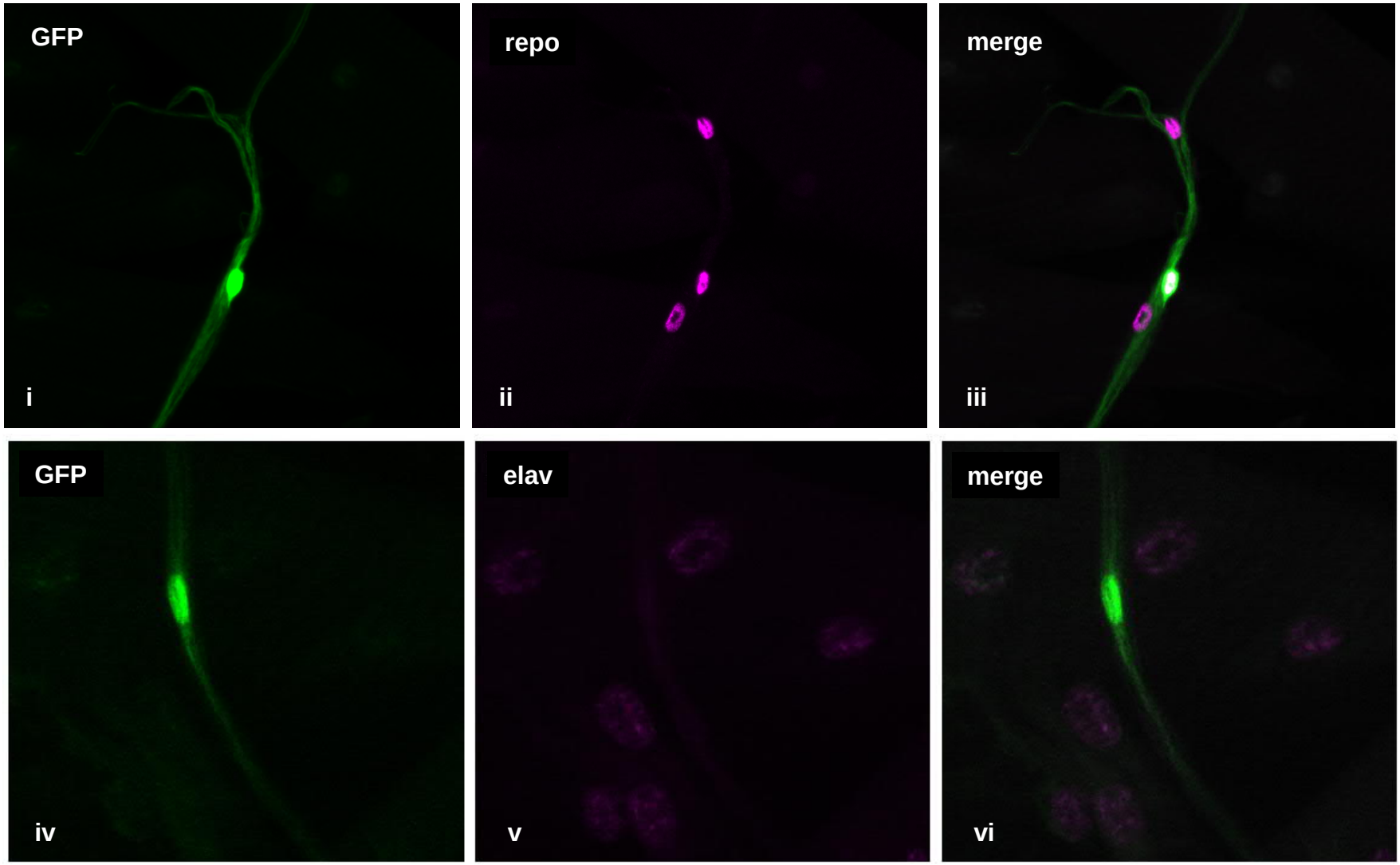

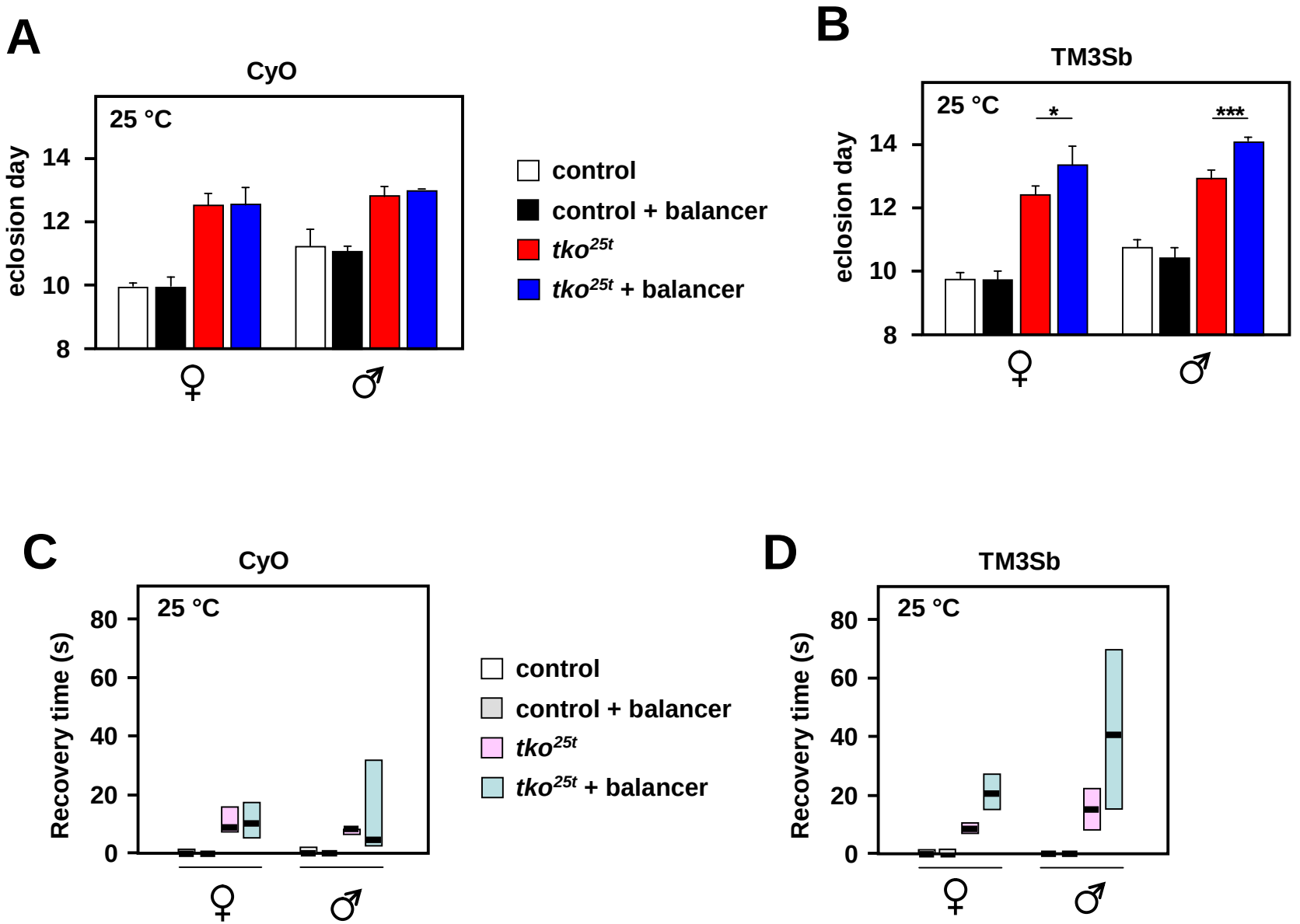

George et al, Figure S2

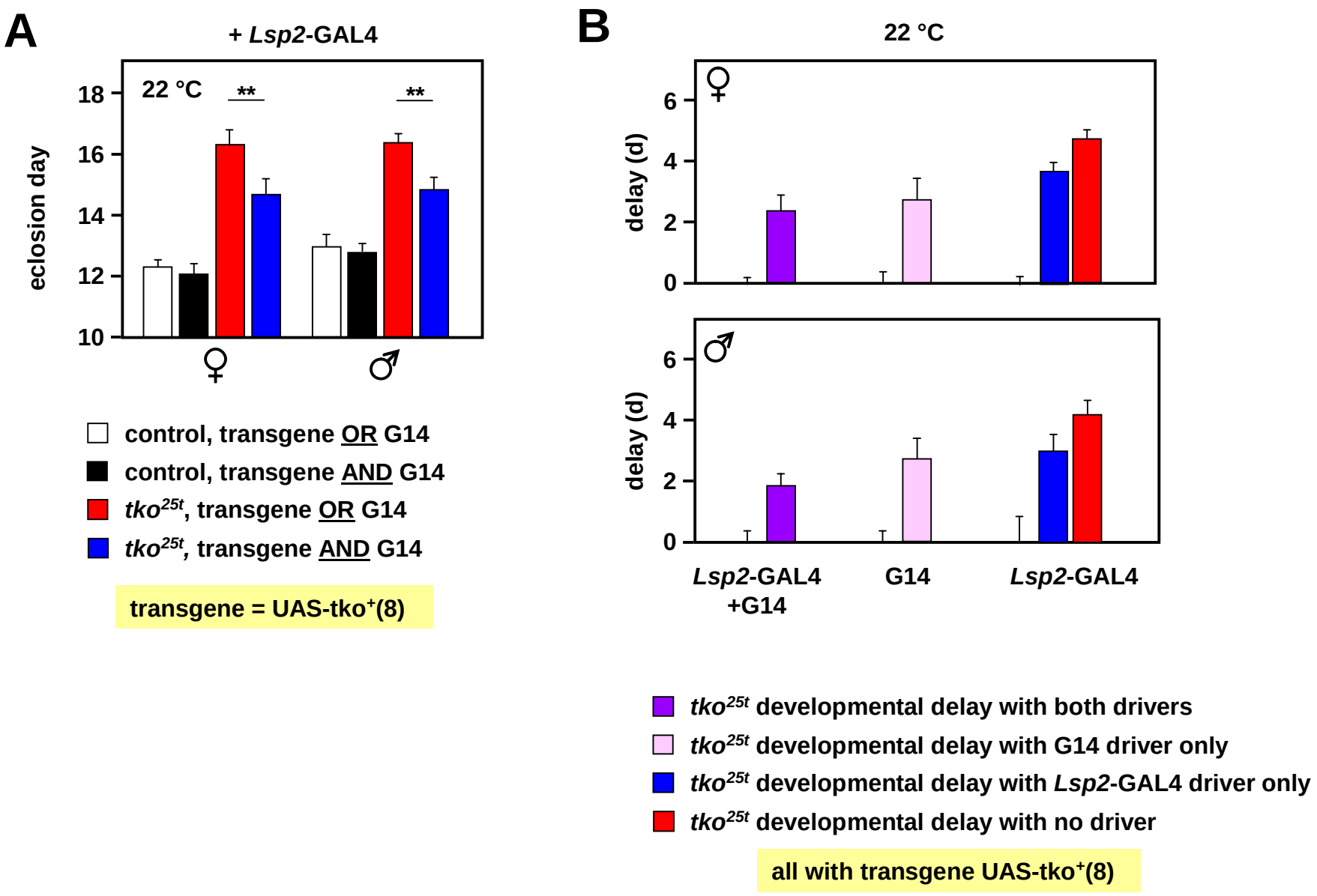

George et al, Figure S3

A

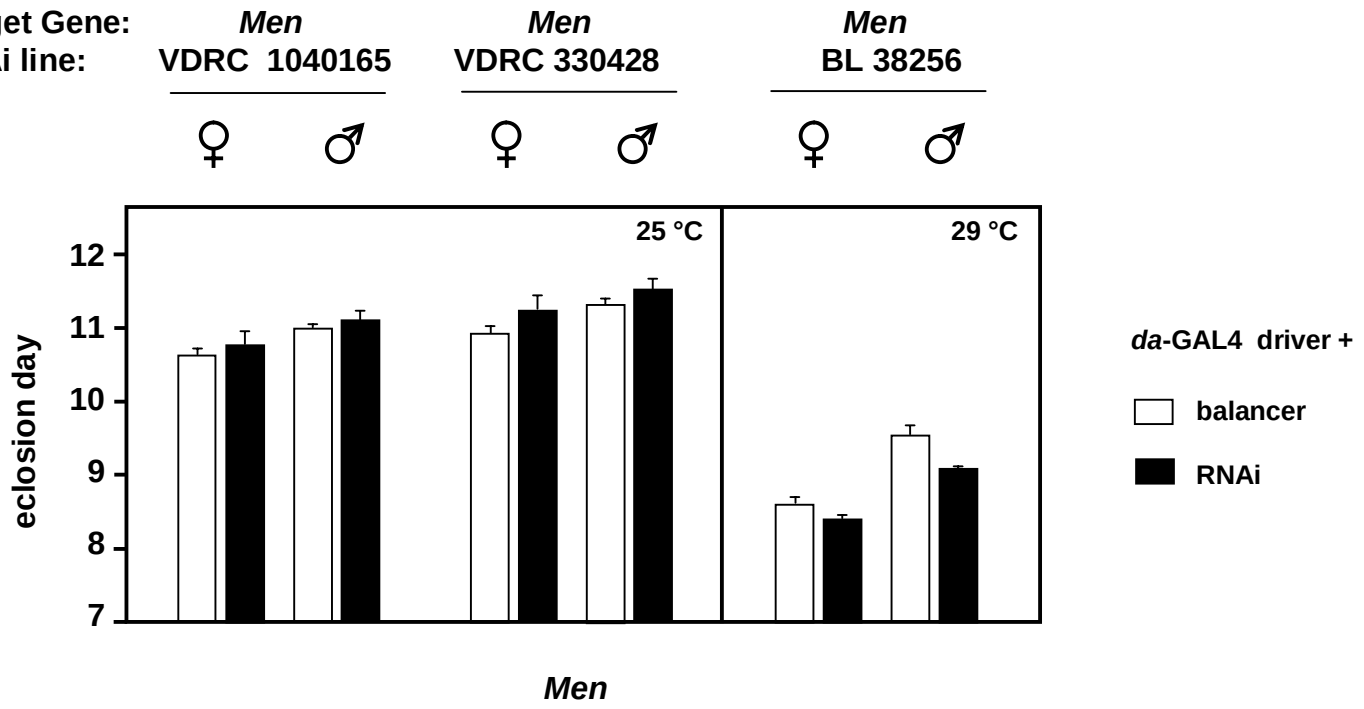
Target Gene:
RNAi line:
Men
VDRC 1040165
Men
VDRC 330428
Men
BL 38256
♀
♂
♀
♂
♀
♂
25 °C
29 °C
eclosion day
12
11
10
9
8
7
Men
da-GAL4 driver +
balancer
RNAi

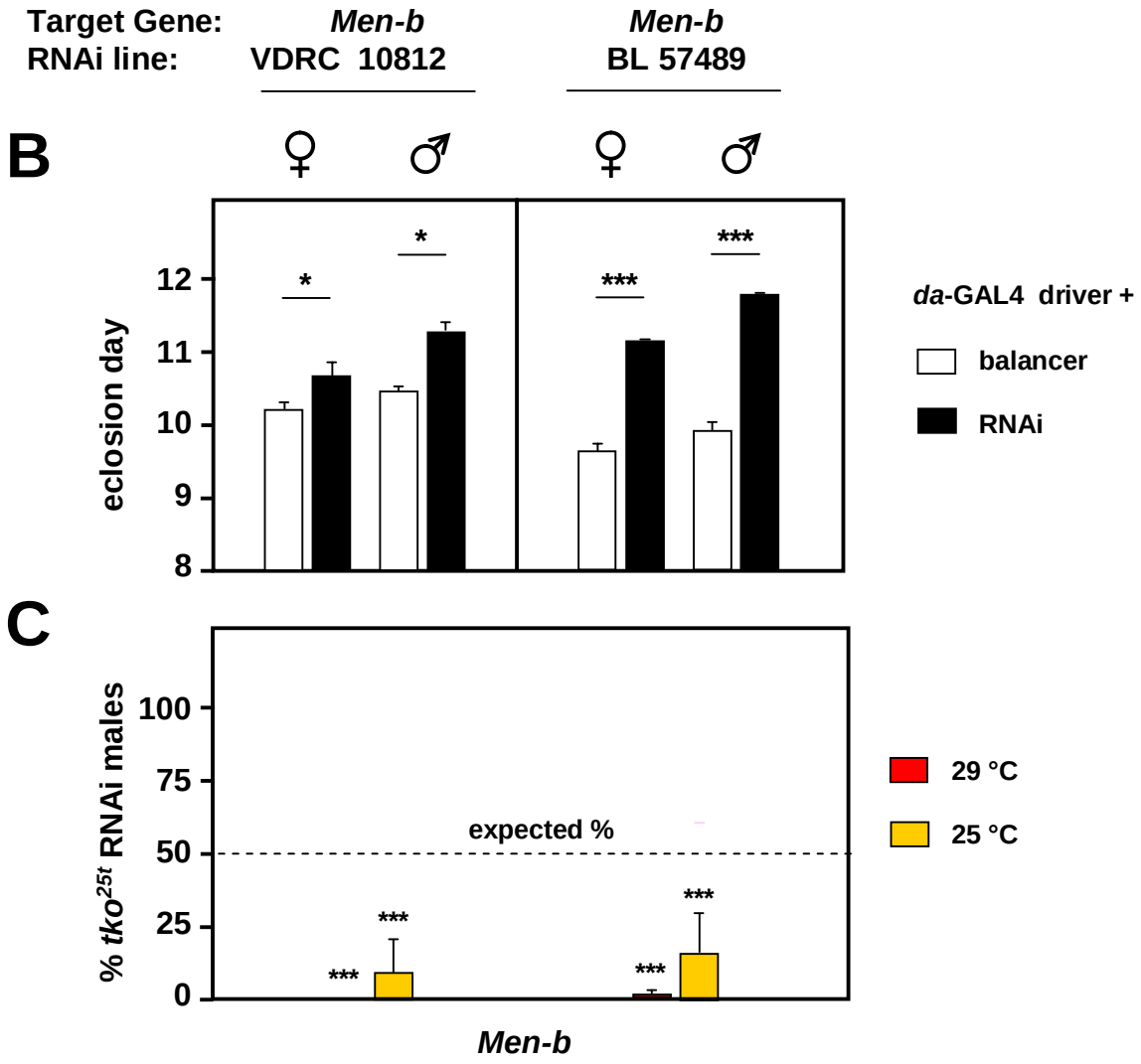
Target Gene:
Men-b
Men-b
RNAi line:
VDRC 10812
BL 57489
B
♀
♂
♀
♂
eclosion day
12
11
10
9
8
*
*
***
***
da-GAL4 driver +
balancer
RNAi
C
% tko25t RNAi males
100
75
50
25
0
expected %
***
***
***
***
29 °C
25 °C
Men-b

FIGURE S5 – Analysis of Figure 5A

HS males

ANOVA Summary					
Source	SS	df	MS	F	P
Genotype	238.3	1	238.3	860.12	<.0001
Drug	13.25	3	4.42	15.94	<.0001
Interaction	4.04	3	1.35	4.86	0.0048
Error	14.13	51	0.28		
Total	330.71	58			

Critical Values for the Tukey HSD Test		
	HSD[.05]	HSD[.01]
Genotype	0.28	0.37
Drug	0.59	0.73
Interaction	1.01	1.19

Results of HSD test

Significance classes by drug only ($p < 0.05$):

no drug	a
pyruvate	b
DCA	b
UK-5099	b

Significance classes for interaction ($p < 0.05$):

no drug, Oregon R	a
no drug, *tko*^{25t}	b
pyruvate, Oregon R	c
pyruvate, *tko*^{25t}	d
DCA, Oregon R	c
DCA, *tko*^{25t}	d
UK-5099, Oregon R	a,c
UK-5099, *tko*^{25t}	d

HS females

ANOVA Summary					
Source	SS	df	MS	F	P
Genotype	197.67	1	197.67	837.31	<.0001
Drug	14.83	3	4.94	20.93	<.0001
Interaction	4	3	1.33	5.65	0.002
Error	12.04	51	0.24		
Total	282.9	58			

Critical Values for the Tukey HSD Test		
	HSD[.05]	HSD[.01]
Genotype	0.25	0.34
Drug	0.55	0.68
Interaction	0.93	1.1

Results of HSD test

Significance classes by drug only ($p < 0.05$):

no drug	a
pyruvate	b
DCA	b
UK-5099	b

Significance classes for interaction ($p < 0.05$):

no drug, Oregon R	a
no drug, *tko*^{25t}	b
pyruvate, Oregon R	c
pyruvate, *tko*^{25t}	d
DCA, Oregon R	c
DCA, *tko*^{25t}	d
UK-5099, Oregon R	a,c
UK-5099, *tko*^{25t}	d

ZS males

ANOVA Summary					
Source	SS	df	MS	F	P
Genotype	54.32	1	54.32	211.56	<.0001
Drug	16.36	2	8.18	31.86	<.0001
Interaction	1.26	2	0.63	2.46	0.1005
Error	8.73	34	0.26		
Total	100.12	39			

Critical Values for the Tukey HSD Test		
	HSD[.05]	HSD[.01]
Genotype	0.33	0.44
Drug	0.51	0.65
Interaction	0.89	1.08

Results of HSD test

Significance classes by drug only ($p < 0.05$):

no drug	a
pyruvate	b
DCA	c

ZS females

ANOVA Summary					
Source	SS	df	MS	F	P
Genotype	41.5	1	41.5	218.77	<.0001
Drug	16.04	2	8.02	42.27	<.0001
Interaction	3.6	2	1.8	9.48	0.0005
Error	6.45	34	0.19		
Total	85.33	39			

Critical Values for the Tukey HSD Test		
	HSD[.05]	HSD[.01]
Genotype	0.28	0.38
Drug	0.44	0.56
Interaction	0.77	0.93

Results of HSD test

Significance classes by drug only ($p < 0.05$):

no drug	a
pyruvate	b
DCA	c

Significance classes for interaction ($p < 0.05$):

no drug, Oregon R	a
no drug, *tko*^{25t}	b
pyruvate, Oregon R	c
pyruvate, *tko*^{25t}	d
DCA, Oregon R	c
DCA, *tko*^{25t}	b,d

FIGURE S6 – Analysis of Figure 6B

Figure 6Bi – Mpc1

HS males

ANOVA Summary					
Source	SS	df	MS	F	P
genotype	63.43	1	63.43	737.61	<.0001
RNAi	0.38	1	0.38	4.43	0.0526
interaction	0.47	1	0.47	5.48	0.0335
Error	1.29	15	0.09		
Total	67.11	18			

Critical Values for the Tukey HSD Test		
	HSD[.05]	HSD[.01]
genotype	0.29	0.4
RNAi	0.29	0.4
interaction	0.55	0.71

Results of HSD test

Significance classes ($p < 0.05$):

Oregon R	a
tko^{25t}	b
Oregon R + RNAi	a
tko^{25t} + RNAi	c

HS females

ANOVA Summary					
Source	SS	df	MS	F	P
genotype	50.05	1	50.05	1195.33	<.0001
RNAi	0	1	0	0.01	0.9216
interaction	0.22	1	0.22	5.37	0.0341
Error	0.67	16	0.04		
Total	50.95	19			

Critical Values for the Tukey HSD Test		
	HSD[.05]	HSD[.01]
genotype	0.19	0.27
RNAi	0.19	0.27
interaction	0.37	0.48

Results of HSD test

Significance classes ($p < 0.05$):

Oregon R	a
tko^{25t}	b
Oregon R + RNAi	a
tko^{25t} + RNAi	b

HS+pyr males

ANOVA Summary					
Source	SS	df	MS	F	P
genotype	14.51	1	14.51	172.75	<.0001
RNAi	1.14	1	1.14	13.56	0.0022
interaction	0.95	1	0.95	11.34	0.0042
Error	1.26	15	0.08		
Total	18.05	18			

Critical Values for the Tukey HSD Test		
	HSD[.05]	HSD[.01]
genotype	0.28	0.39
RNAi	0.28	0.39
interaction	0.55	0.7

Results of HSD test

Significance classes ($p < 0.05$):

Oregon R	a
tko^{25t}	b
Oregon R + RNAi	c
tko^{25t} + RNAi	b

HS+pyr females

OVA Summary					
Source	SS	df	MS	F	P
genotype	16.25	1	16.25	119.85	<.0001
RNAi	1.88	1	1.88	13.85	0.0019
interaction	0.7	1	0.7	5.13	0.0378
Error	2.17	16	0.14		
Total	21	19			

Critical Values for the Tukey HSD Test		
	HSD[.05]	HSD[.01]
genotype	0.35	0.48
RNAi	0.35	0.48
interaction	0.67	0.86

Results of HSD test

Significance classes ($p < 0.05$):

Oregon R	a
tko^{25t}	b
Oregon R + RNAi	c
tko^{25t} + RNAi	b

Figure 6Bii – Pdk

HS males

ANOVA Summary					
Source	SS	df	MS	F	P
genotype	80.8	1	80.8	618.58	<.0001
RNAi	0.08	1	0.08	0.63	0.439
interaction	0.04	1	0.04	0.3	0.5914
Error	2.09	16	0.13		
Total	83.01	19			

Critical Values for the Tukey HSD Test		
	HSD[.05]	HSD[.01]
genotype	0.34	0.47
RNAi	0.34	0.47
interaction	0.65	0.84

HS females

ANOVA Summary					
Source	SS	df	MS	F	P
genotype	63.4	1	63.4	805.13	<.0001
RNAi	0.14	1	0.14	1.77	0.202
interaction	0	1	0	0.01	0.9216
Error	1.26	16	0.08		
Total	64.8	19			

Critical Values for the Tukey HSD Test		
	HSD[.05]	HSD[.01]
genotype	0.27	0.37
RNAi	0.27	0.37
interaction	0.51	0.65

HS+pyr males

ANOVA Summary					
Source	SS	df	MS	F	P
genotype	16.99	1	16.99	245.4	<.0001
RNAi	0.38	1	0.38	5.43	0.0365
interaction	0.36	1	0.36	5.23	0.0396
Error	0.9	13	0.07		
Total	18.36	16			

Critical Values for the Tukey HSD Test		
	HSD[.05]	HSD[.01]
genotype	0.28	0.39
RNAi	0.28	0.39
interaction	0.57	0.75

Results of HSD test

Significance classes ($p < 0.05$):

Oregon R	a
tko^{25t}	b
Oregon R + RNAi	a
tko^{25t} + RNAi	c

HS+pyr females

ANOVA Summary					
Source	SS	df	MS	F	P
genotype	12.14	1	12.14	183.48	<.0001
RNAi	0.41	1	0.41	6.17	0.0274
interaction	0.86	1	0.86	12.93	0.0033
Error	0.86	13	0.07		
Total	13.11	16			

Critical Values for the Tukey HSD Test		
	HSD[.05]	HSD[.01]
genotype	0.27	0.38
RNAi	0.27	0.38
interaction	0.56	0.73

Results of HSD test

Significance classes ($p < 0.05$):

Oregon R	a
tko^{25t}	b
Oregon R + RNAi	a
tko^{25t} + RNAi	c